Thermochimica Acta 494 (2009) 86–93

Contents lists available at ScienceDirect

Thermochimica Acta

journal homepage: www.elsevier.com/locate/tca

In situ high-temperature Mössbauer spectroscopic study of carbon nanotube–Fe–Al_2O_3 nanocomposite powder

Valdirene G. de Resende [a,b,*], Alain Peigney [b], Eddy De Grave [a], Christophe Laurent [b]

[a] Department of Subatomic and Radiation Physics, University of Ghent, B-9000 Gent, Belgium
[b] Université de Toulouse, Institut Carnot CIRIMAT, CNRS-UPS, Université Paul-Sabatier, Bât. 2R1, 118 route de Narbonne, 31062 Toulouse cedex 9, France

ARTICLE INFO

Article history:
Received 4 March 2009
Received in revised form 27 April 2009
Accepted 28 April 2009
Available online 5 May 2009

Keywords:
Carbon nanotubes
Thermal stability
Electron microscopy
Mössbauer spectroscopy

ABSTRACT

The oxidation of a carbon nanotube–Fe–Al_2O_3 nanocomposite powder was investigated using notably thermogravimetric analysis, room temperature transmission and emission Mössbauer spectroscopy and, for the first time, *in situ* high-temperature transmission Mössbauer spectroscopy. The first weight gain (150–300 °C) was attributed to the oxidation into hematite of the α-Fe and Fe_3C particles located at the surface and in the open porosity of the alumina grains. The 25 nm hematite particles are superparamagnetic at 250 °C or above. A weight loss (300–540 °C) corresponds to the oxidation of carbon nanotubes and graphene layers surrounding the nanoparticles. The graphene layers surrounding γ-Fe–C particles are progressively oxidized and a very thin hematite layer is formed at the surface of the particles, preventing their complete oxidation while helping to retain the face-centered cubic structure. Finally, two weight gains (670 and 1120 °C) correspond to the oxidation of the intragranular α-Fe particles and the γ-Fe–C particles.

1. Introduction

Although many studies on the thermal stability of samples of carbon nanotubes (CNT) have been reported, most of them are performed on purified specimens and focus on the oxidation of the CNTs. By contrast, relatively few thermal stability studies have been reported on the as-produced specimens, i.e. still containing the catalyst and substrate [1–5] or on CNT–oxides mixtures prepared on purpose [6,7]. The synthesis of CNTs by catalytic chemical vapor deposition (CCVD) is based on the catalytic decomposition of carbonaceous gases on transition metal nanoparticles which quite often are made up of iron, iron-cobalt, iron-nickel or iron-molybdenum alloys or mixtures. ^{57}Fe Mössbauer spectroscopy (MS) offers several advantages for studies of iron-containing compounds. The spectra, and parameters derived from these, are very sensitive to electronic, magnetic and structural characteristics of the probed material and as such, MS is a useful tool for phase identification and quantification of mixtures of Fe-bearing materials. The aim of this paper is to study the oxidation in air of a CNT–Fe–Al_2O_3 nanocomposite powder using notably thermogravimetric analysis and, for the first time to the best of our knowledge, *in situ* high temperature MS to follow the evolution of the various iron phases in the different stages of the oxidation process of the nanocomposite powder.

2. Experimental

2.1. Materials

A CNT–Fe–Al_2O_3 nanocomposite powder (henceforward codenamed as C0) was obtained by the reduction of an α-$(Al_{0.93}Fe_{0.07})_2O_3$ powder in a H_2–CH_4 gas mixture as described elsewhere [8]. Briefly, the α-$(Al_{0.93}Fe_{0.07})_2O_3$ powder was prepared by decomposition and calcination of the mixed oxinate precursors. The powder is made up of 2–5 μm grains assembled into tabular-like aggregates presenting the porous vermicular microstructure with much looser aggregates made up of 0.2–0.5 μm primary grains or crystallites. The powder was reduced in a H_2–CH_4 (20 mol% CH_4) gas mixture. The heating and the cooling rate to the desired temperature (1025 °C) and back to room temperature was 5 °C/min. No dwell time was applied at 1025 °C. The so-obtained CNT–Fe–Al_2O_3 nanocomposite powder was studied in detail by a variety of techniques [8] the results of which are summarized in the following. The carbon content (C_n) was found equal to 1.6 wt.%. The ratio between the intensity of the D band (*ca.* 1320 cm^{-1}) and the G band (*ca.* 1580 cm^{-1}) of the high-frequency range of the Raman spectra, $I_{D/G}$, is equal to about 30%. An increasing $I_{D/G}$ value corresponds to a higher proportion of sp^3-like carbon, which is generally

* Corresponding author at: Department of Subatomic and Radiation Physics, University of Ghent, Division NUMAT, Proeftuinstraat 86, B-9000 Gent, Belgium. Fax: +32 09 264 6697.
E-mail address: Valdirene.Gonzaga@Ugent.be (V.G. de Resende).

0040-6031/$ – see front matter © 2009 Elsevier B.V. All rights reserved.
doi:10.1016/j.tca.2009.04.024

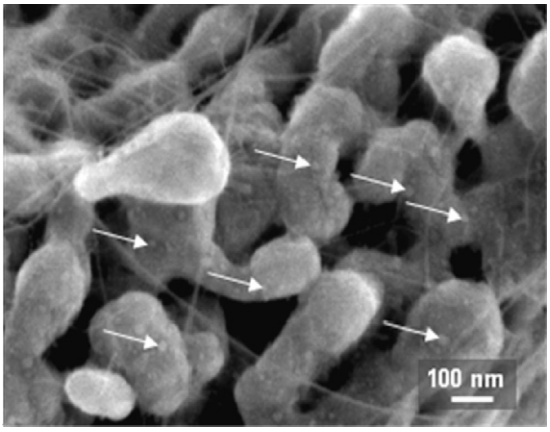

Fig. 1. Typical FEG-SEM image of the CNT–Fe–Al_2O_3 nanocomposite powder. The arrows point α-Fe, Fe_3C and/or γ-Fe–C nanoparticles at the surface of the alumina grains.

attributed to the presence of more structural defects. The presence of radial-breathing-modes (RBM) peaks in the low-frequency range (100–300 cm^{-1}) of the spectrum, the frequencies of which are inversely proportional to the CNT diameters, reveals the presence of small-diameter CNTs, such as SWNTs and DWNTs. A typical FEG-SEM image of a porous area of the powder (Fig. 1) reveals the presence of long, flexible filaments, with a smooth and regular surface, on the surface of the oxide grains and bridging several grains. All filaments have a diameter smaller than 30 nm and a length of the order of some tens of micrometers. From earlier results, it is known that such filaments are isolated CNTs and/or CNTs bundles. Spherical particles 5–20 nm in diameter, that may be α-Fe, Fe_3C and/or γ-Fe–C (some of which are arrowed in Fig. 1) are observed at the surface of the alumina grains. Most of these particles are covered by a few graphene layers and do not appear to be connected to a CNT, indicating that they have been inactive for the formation of CNT. It is interesting to note that the presence of undesirable thick, short carbon nanofibers is rarely observed.

2.2. Methods

Thermogravimetric analysis (TGA) of the CNT–Fe–Al_2O_3 nanocomposite powder was performed in a SETARAM TAG 24 module (simultaneous symmetrical thermoanalyser). The powder (~22 mg) was heated (1 °C/min) from 25 to 1300 °C in a constant flow of synthetic air (1.5 l/h). Based on the TGA curve, parts of the nanocomposite powder (~400 mg) were heated (1 °C/min) in a tubular furnace in flowing air at selected temperatures between 250 and 1300 °C. Immediately after the furnace has reached the desired temperature, the powders were quenched in air. The oxidized powders are hereafter named as C followed by the respective temperature of oxidation (for instance sample C250 is a powder heated at 250 °C).

XRD patterns were recorded in the range 10–70° (2θ) using a Bruker D4 Endeavor diffractrometer equipped with a Cu Kα radiation tube. Counts were registered every 0.02° (2θ). The carbon content (C_n) was measured by the flash combustion method (the accuracy of the measurements is ±2%). The powders were observed by FEG-SEM (JEOL JSM 6700F), with an acceleration tension of 5 kV using the in-lens electron detector.

All powders were studied by transmission Mössbauer spectroscopy (TMS), integral low-energy electron Mössbauer spectroscopy (ILEEMS) and *in situ* high-temperature transmission Mössbauer spectroscopy (HTTMS). TMS is used to study the bulk of the material while ILEEMS is applied to examine the surface of the powders. HTTMS spectra were recorded to obtain *in situ* information about the oxidation processes of the CNT nanocomposite powder and to identify and quantify the oxidation products formed. At room temperature (25 °C) both TMS and ILEEMS were employed. HTTMS was applied at selected temperatures between 25 and 850 °C. The spectrometers were operating at constant acceleration mode with triangular reference signals. ^{57}Co(Rh) sources were used. All Mössbauer spectra were analyzed in terms of model-independent distributions of hyperfine-parameter values and numerical data quoted hereafter refer to maximum-probability values. Isomer shifts are referenced with respect to α-Fe at room temperature. ILEEMS is a variant of Mössbauer spectroscopy in which low-energy electrons are counted. The majority of these electrons, with energy of ~10 eV, are produced by after effects following the decay of the probe nuclei in an extremely thin surface layer of the absorber. Consequently, by comparing the ILEEMS results with those of TMS, information of the surface of the material can be inferred [9]. The HTTMS measurements were performed using a furnace (Wissel Scientific Instruments, model MBF-1100) in which a constant gas flow of either synthetic air or N_2 was maintained. The furnace was heated at 1 °C/min under flow of synthetic air. After the furnace had reached the desired temperature the gas flow was switched to N_2 to avoid further oxidation of the powder. The N_2 flow was kept during the acquisition of the spectrum. With the spectrum containing enough statistics the flow was switched back to synthetic air and the temperature was increased at 1 °C/min up to the next desired temperature. The gas flow was then switched back to N_2 in order to collect the next spectrum. These steps were done consecutively until the furnace reached the maximum desired temperature (850 °C). Immediately after having recorded the spectrum at 850 °C, the flow of N_2 was switched to air and the furnace was cooled down to room temperature at natural cooling of the furnace. Subsequently a final spectrum was collected at 25 °C.

3. Results and discussion

The TGA curve and the corresponding derivative curve (DTG) (Fig. 2) show several steps, involving both weight losses and gains at different stages. The initial weight loss at temperatures below

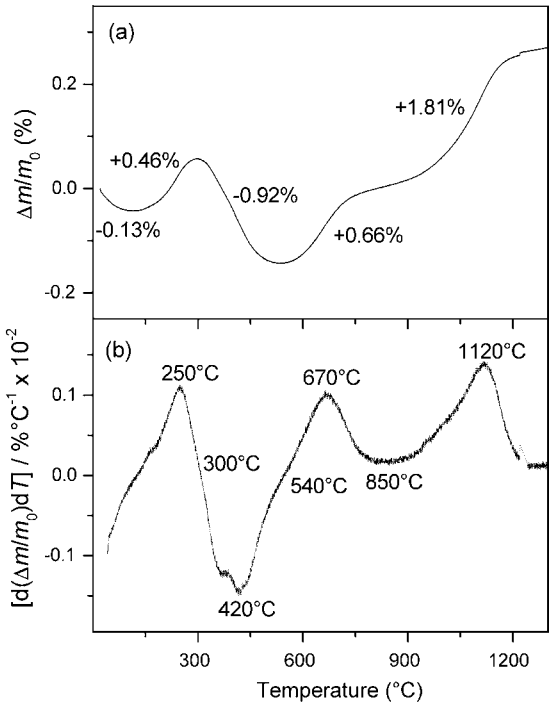

Fig. 2. TGA (a) and DTG (b) curves for the CNT–Fe–Al_2O_3 nanocomposite powder.

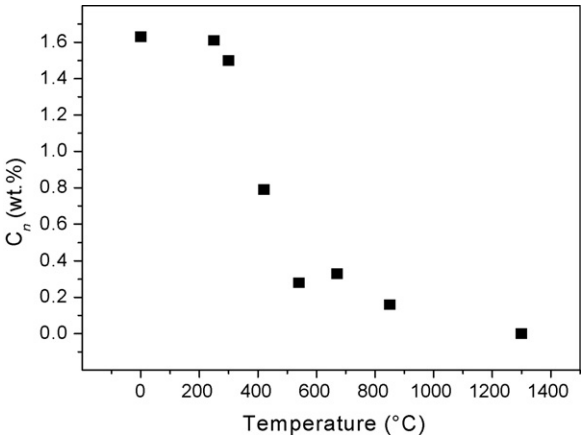

Fig. 3. Carbon content versus the increase in calcination temperature.

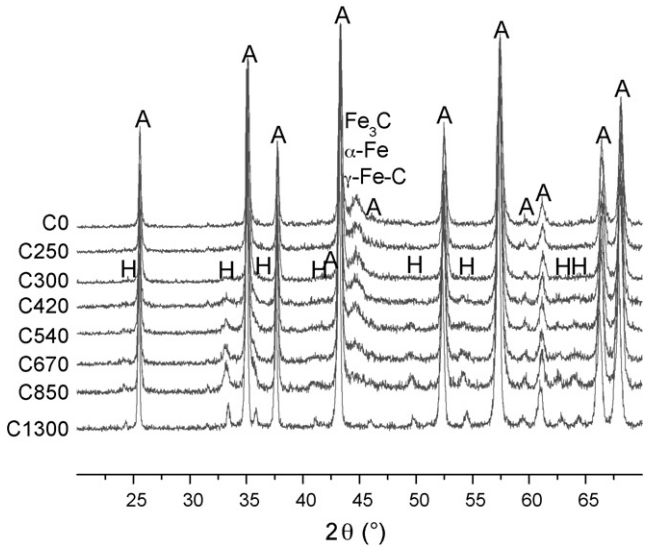

Fig. 4. XRD patterns of the calcined powders. A: α-Al_2O_3 and H: α-Fe_2O_3.

150 °C is attributed to desorption, mostly corresponding to species adsorbed onto the surface of the CNTs. A weight gain is observed in the range 150–300 °C. According to earlier studies [10], this weight gain could correspond to the oxidation of the Fe and Fe-carbide particles located at the surface and in the open porosity of the alumina grains. A second weight loss (−0.92%) is observed in the range 300–540 °C. This weight loss is supposed [1] to be due to the oxidation of carbon, free or combined with iron. The DTG curve suggests that this process actually proceeds in two steps, which could indeed indicate the successive oxidation of different forms of carbon. However, the two steps are ill-resolved and sound conclusions in that respect cannot be drawn. Interestingly, Mössbauer spectroscopy results (see later in this section) indicate that γ-Fe–C particles have not been oxidized at these temperatures. At temperatures increasing beyond 540 °C, two successive weight gains are observed (DTG peaks at 670 and 1120 °C). From earlier results on carbon-free metal-oxide powders [10,11], both weight gains are proposed to correspond to the oxidation of intragranular α-Fe particles. However, Mössbauer spectroscopy results (see later in this section) could indicate that the 1120 °C peak also involve γ-Fe–C particles and a $FeAl_2O_4$ phase.

On the basis on the TGA curve discussed above, batches of the CNT–Fe–Al_2O_3 nanocomposite powder were calcined in air at 250, 300, 420, 540, 670, 850, and 1300 °C. The carbon content C_n was found to gradually decrease from 1.6 to 0.2 wt.% as the calcination temperature is increased to 850 °C (Fig. 3). For C1300, C_n is below 0.2 wt.%, which is within the detection limit of the technique. A comparison can be made between the second weight loss measured in the TGA (−0.92%) and that corresponding to the change in carbon content from room temperature to 540 °C (−1.35%), the latter being significantly higher. This shows that the first weight gain and the second weight loss are superimposed and thus, it is not possible to extract from the TGA curve quantitative results neither for determining the contents of different carbon forms nor for assessing the oxidation yield of iron species in this temperature range (about 200–540 °C).

Analyses of the XRD patterns for C0–C540 (Fig. 4) reveal the presence of α-Fe and/or Fe_3C (cementite) besides the α-alumina matrix. It is, however, difficult to discriminate between the patterns of α-Fe and Fe_3C because the respective diffraction peaks are strongly overlapping. γ-Fe may also be present in the powders, but it cannot be resolved from the XRD patterns because its main (1 1 1) diffraction peak (d_{111} = 0.208 nm) is probably masked by the α-alumina peak (d_{113} = 0.209 nm). The intensity of the α-Fe and Fe_3C peaks regularly decreases upon the increase in calcination temperature above 540 °C (C670 and C850). These peaks are no longer detected for C1300. From C300 to C850, hematite (α-Fe_2O_3) peaks are detected with increasing intensity. For C1300, the hematite peaks appear to be slightly less intense than for C850, which could indicate a partial dissolution into alumina.

Typical FEG-SEM micrographs for selected powders are shown in Fig. 5. It is difficult from such images to distinguish C0 (Fig. 5a), C250 (not shown), C300 (Fig. 5b) and C420 (Fig. 5c) from each other. Indeed, CNTs, CNT bundles and 15–30 nm nanoparticles located at the surface at the alumina grains are observed. By contrast, much less CNTs and CNT bundles are observed for C540 (Fig. 5d) and C670 (Fig. 5e). Moreover, for C670, a high density of nanoparticles with a uniform diameter (∼20 nm) is observed. For C850 (not shown), CNTs are extremely rarely observed and for C1300 (Fig. 5f), no CNTs are observed. Interestingly, for C1300, no surface nanoparticles are observed. This could support the XRD result that hematite particles are dissolved into alumina after the treatment in air at 1300 °C.

The TMS recorded at 25 °C for all powders are reproduced in Fig. 6. Each spectrum in general was fitted as a superposition of different subspectra: an outer sextet due to α-Fe_2O_3, a middle sextet accounting for α-Fe, an inner sextet representing Fe_3C, a singlet characteristic of γ-Fe–C, an Fe^{3+} doublet ascribed to iron ions in the structure of α-Al_2O_3 (noted as $(Al,Fe)_2O_3$) and an Fe^{2+} doublet that reflects the presence of small amount of hercynite ($FeAl_2O_4$). Note that the α-Fe_2O_3 sextet was not present for C0. For C670 and C850, no Fe_3C component was resolvable, and for C1300 only the α-Fe_2O_3 sextet and the ferric doublet were found to exist. Consistently, the most adequate fits of the TMS were obtained assuming hyperfine-parameter distributions for all components, hereby imposing a 3:2:1 ratio for the relative spectral areas of outer lines to middle lines to inner lines for the elemental sextets. The respective Mössbauer parameter values obtained from the data reductions are listed in Table 1. The presence of both the Fe^{3+} and Fe^{2+} doublets for C0 are due to the incomplete reduction of the solid solution. The remaining Fe^{3+} ions are deep within the alumina grains and it is possible that the Fe^{2+} ions correspond to a very thin (<5 nm) layer of $FeAl_2O_4$ surrounding some intragranular Fe nanoparticles, which has been observed before [12]. Note that the proportion of Fe^{2+} ions is not affected by heating at temperatures as high as 850 °C (Table 1), which support the hypothesis that the corresponding species are within the alumina grains. The relative spectral area (RA) of the hematite component gradually increases from 0% (C0) to 32% (C850), but exhibits a sudden drop to 19% for C1300. This indicates that the hematite particles have been partly dissolved into alumina in agreement with the above XRD and

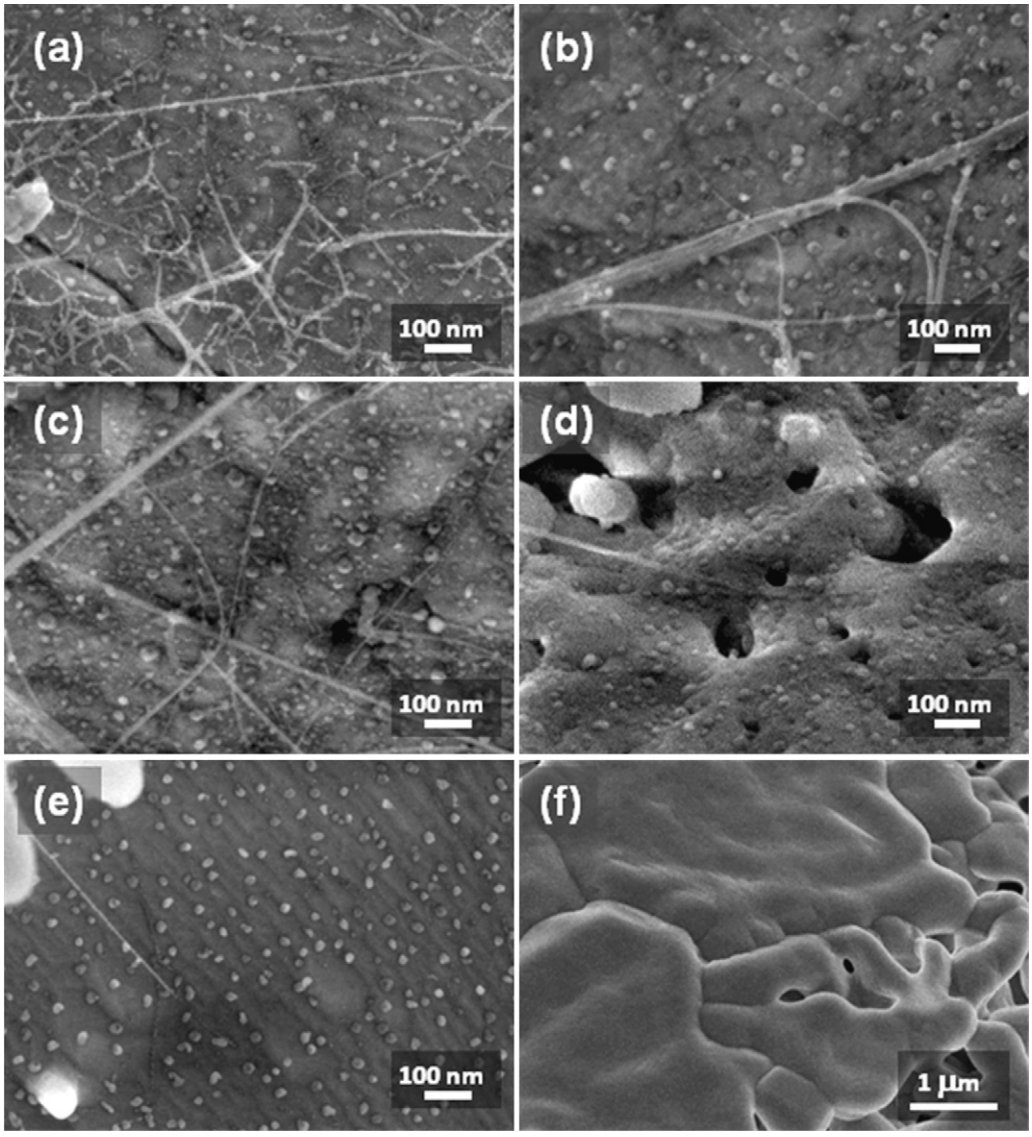

Fig. 5. Typical FEG-SEM images of the calcined powders: (a) C0; (b) C300; (c) C420; (d) C540; (e) C670; (f) C1300.

FEG-SEM results. The α-Fe contribution gradually decreases from 30% (C0) to 12% (C850), traducing the oxidation of the surface α-Fe particles, as opposed to the intragranular ones, and thus partly accounting for the increase of the hematite proportion. As mentioned above, no α-Fe is detected for C1300, the intragranular α-Fe particles having been oxidized too. A gradual decrease of the Fe_3C proportion upon raising the calcination temperature is observed, from 21% (C0) to 6% (C540). For C670 onwards, no Fe_3C is detected. Considering the respective proportion of α-Fe, Fe_3C and α-Fe_2O_3 (Table 1), it appears clearly that both α-Fe and Fe_3C are gradually oxidized into α-Fe_2O_3 as the calcination temperature is increased to 850 °C. By contrast, and surprisingly, the proportion of γ-Fe–C is not affected by heating at temperatures as high as 850 °C (Table 1). Kim and Sigmund [13] reported on large γ-Fe particles (100 nm in diameter) tightly encapsulated by a graphitic film. These authors inferred that the graphitic film prevents the γ-Fe from transforming into α-Fe (the stable phase of iron at room temperature). The study of the present powder by high-resolution transmission electron microscopy revealed the presence of encapsulated particles with diameters of 15–20 nm [8], which were too large for being active for the formation of CNTs and ended up covered by several graphene layers. Therefore, it is not unreasonable to propose that these are the γ-Fe–C particles and that after the oxidation of the graphene layers covering them, a very thin layer of α-Fe_2O_3 is formed at their surface, thus preventing a complete oxidation until high temperatures such as 850 °C while helping to retain the face-centered cubic structure. It is well-know that iron particles actively react with oxygen even at room temperature, resulting in an iron oxide layer on the surface of the particles protecting them from further inward oxidation. If this suggestion is indeed reasonable one would then wonder why no change in the area ratio was observed for the γ-Fe–C component (Table 1). The layer of hematite that could be covering the γ-Fe–C particles could be extremely thin so that the measurable abundance is within the experimental error and consequently one cannot observe changes in area ratio in the TMS. Indeed, De Grave et al. [9] observed by ILEEMS that very thin layers of α-Fe_2O_3 on Fe-containing particles are not detected by TMS.

ILEEMS experiments at 25 °C were carried out to examine whether the surface of the powder is affected differently by the heating as compared to the bulk. The emission spectra (not shown) clearly exhibit the same shapes and in general the same spectral components as do the corresponding TMS spectra. This indicates that the different iron species are distributed evenly in the bulk and the top most surface of the grains. However, the relative area

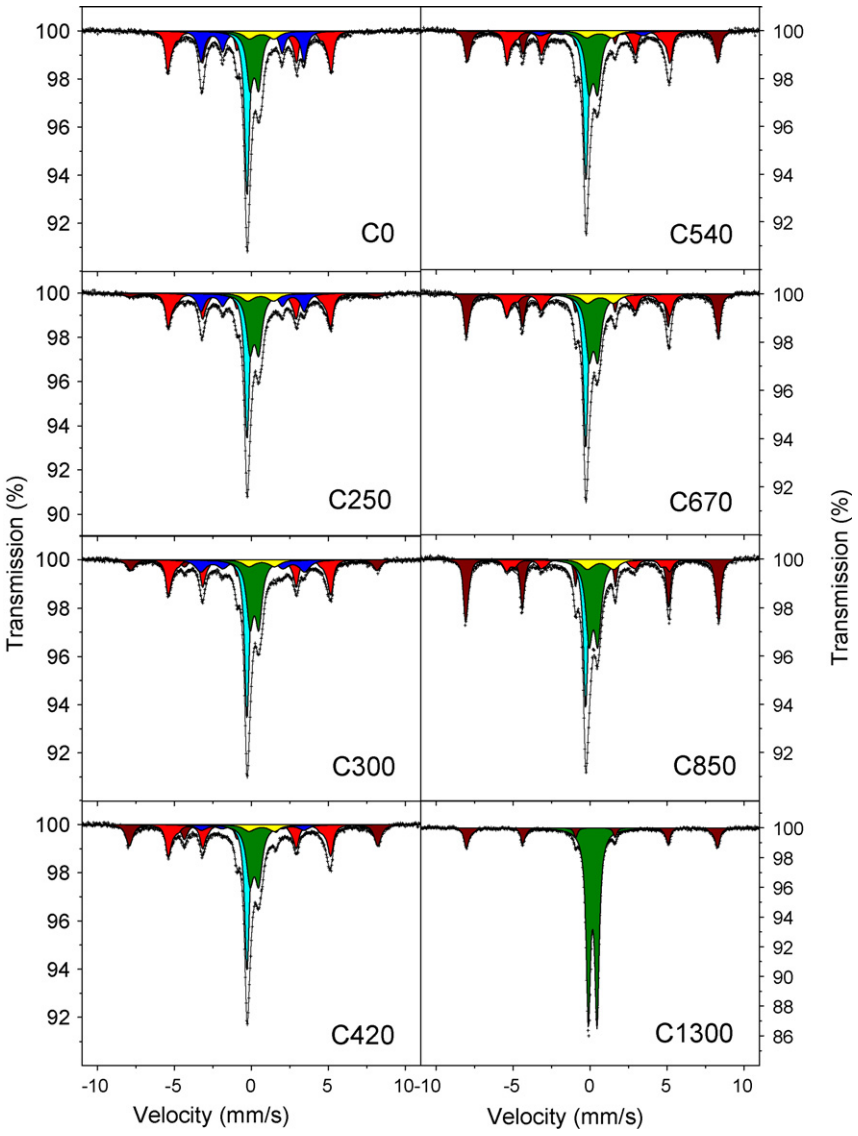

Fig. 6. TMS spectra (collected at 25 °C) of the calcined powder. Solid envelops are the results of fitting the experimental data by model-independent hyperfine-parameter distributions. α-Fe (red); Fe_3C (blue); α-Fe_2O_3 (brown); Fe^{3+} in $(Al,Fe)_2O_3$ (green); Fe^{2+} in $FeAl_2O_4$ (yellow); γ-Fe–C (cyan). (For interpretation of the references to color in this figure legend, the reader is referred to the web version of the article.)

parameter RA for the hematite component in the ILEEMS spectrum of C250 is significantly higher than the corresponding value for the TMS spectrum (13% versus 6%, respectively). Concurrently the contribution of the α-Fe component has dropped to 19% from 27%. This finding suggests that the initial weight gain (250–300 °C) observed in the TGA curve is due to oxidation of the topmost (5 nm) surface α-Fe particles. More details on ILEEMS studies on similar powders can be found elsewhere [14]. The differences between the present results and those of the earlier ILEEMS study arise because of the different oxidation conditions applied: quenching the powder in air immediately after reaching the maximum desired temperature (present study) or oxidation in air at 600 °C during 2 h [14].

The *in situ* HTTMS spectra of the CNT–Fe–Al_2O_3 nanocomposite powder are reproduced in Fig. 7. Only three or four components were required to fit these spectra adequately: an α-Fe sextet, an $(Al,Fe)_2O_3$ doublet and a γ-Fe–C singlet, as well as, for the spectra collected at 250 and 300 °C, an Fe_3C sextet. The adjusted hyperfine parameter values are listed in Table 2 and are all in line with the corresponding values obtained from the TMS and ILEEMS experiments as described in the preceding sections. Some interesting features emerge from the HTTMS experiments:

(i) the absence of the hematite component in all HTTMS spectra while this component is prominently present in the spectrum recorded for the powder cooled down to room temperature after termination of the 850 °C run;
(ii) the gradual increase of the contribution of the $(Al,Fe)_2O_3$ doublet up to 59% while at the final run at 25 °C only 31% is found, which is close to the value for the parent CNT–Fe–Al_2O_3 nanocomposite powder (C0);
(iii) the vanishing of the Fe_3C subspectrum between 300 and 420 °C while according to the TMS results this phase is still present after heating at 540 °C;
(iv) up to 670 °C, the contribution of α-Fe sextet remains unchanged within experimental error limits, whereas at 850 °C this contribution has decreased from 30% to 21%;
(v) the absence of the $FeAl_2O_4$ phase in all of the HTTMS spectra.

To comment on observations (i) to (v), the authors have collected some relevant RA data in Table 3. They concern on the one hand the percentage of the cementite component, RA_c, and the sum RA_{ha} of the hematite and alumina contributions both as obtained from the 25 °C TMS (data from Table 1). On the other hand, the right

Table 1
Relevant hyperfine parameters for the components present on the TMS spectra acquired at 25 °C for the CNT–Fe–Al_2O_3 nanocomposite powder heated in air at selected temperatures.

Sample	$(Al,Fe)_2O_3$			α-Fe_2O_3				Fe^{2+} doublet		
	ΔE_Q	δ	RA	B_{hf}	$2\varepsilon_Q$	δ	RA	ΔE_Q	δ	RA
C0	0.56	0.30	20	–	–	–	–	1.57	0.79	5
C250	0.57	0.31	23	49.4	−0.16	0.31	6	1.64	0.72	6
C300	0.57	0.31	24	49.5	−0.12	0.34	9	1.64	0.80	5
C420	0.56	0.31	24	50.1	−0.18	0.35	17	1.62	0.79	5
C540	0.56	0.31	23	50.7	−0.18	0.36	20	1.62	0.72	5
C670	0.57	0.33	25	50.9	−0.19	0.36	26	1.66	0.79[a]	6
C850	0.57	0.33	29	51.0	−0.21	0.36	32	1.65	0.79[a]	7
C1300	0.56	0.29	81	50.6	−0.22	0.35	19	–	–	–

Sample	α-Fe			Fe_3C				γ-Fe–C	
	B_{hf}	δ	RA	B_{hf}	$2\varepsilon_Q$	δ	RA	δ	RA
C0	32.9	−0.01	30	20.7	0.01	0.19	21	−0.17	24
C250	32.7	−0.01	27	20.8	0.00	0.19	16	−0.17	22
C300	32.8	0.00	25	20.9	−0.02	0.21	15	−0.17	22
C420	32.7	−0.01	25	20.8	0.03[a]	0.19[a]	7	−0.17	22
C540	32.8	0.00	24	20.8	0.03[a]	0.19[a]	6	−0.17	22
C670	32.8	0.00	21	–	–	–	–	−0.17	22
C850	32.9	−0.01	12	–	–	–	–	−0.17	20
C1300	–	–	–	–	–	–	–	–	–

B_{hf}: hyperfine field at maximum of the distribution (T); $2\varepsilon_Q$: quadrupole shifts (mm/s); ΔE_Q: quadrupole splitting at maximum distribution (mm/s); δ: isomer shifts (mm/s); RA: relative spectral areas (%). The values of isomer shifts are with reference to metallic iron.
[a] Fixed parameters.

part of Table 3 contains the RA values of the cementite and alumina phases, RA_c and RA_a, respectively, calculated from the *in situ* HTTMS (data from Table 2). The sum $RA_c + RA_{ha}$ (TMS) and the sum $RA_c + RA_a$ (HTTMS) remain constant at ~50%, except for the highest temperature of 850 °C at which $RA_c + RA_{ha}$ has increased to 61%. For this latter temperature, the α-Fe contribution has dropped to 21% from the otherwise constant value of ~30% found for the lower temperatures (Table 2). This indicates that part of the α-Fe particles has oxidized, presumably forming α-Fe_2O_3. Hematite is paramagnetic at high temperatures ($T > 668$ °C) and hence gives rise to a doublet with hyperfine parameters that are very similar to those of the present $(Al,Fe)_2O_3$ doublet [15]. As a consequence, the hematite

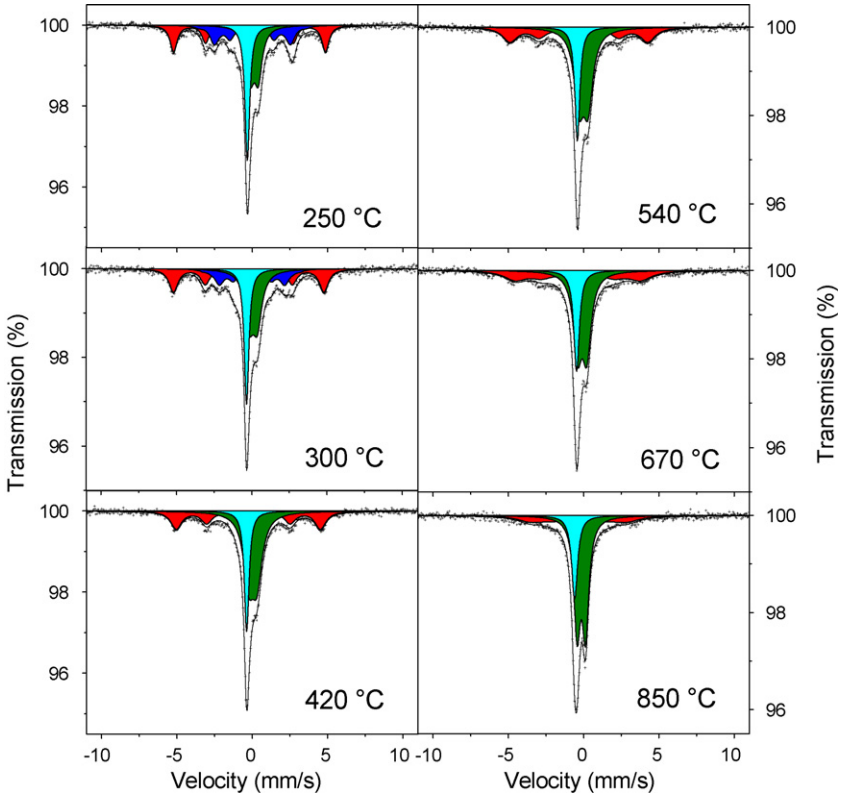

Fig. 7. HTTMS spectra collected at selected temperatures. Solid envelops are the results of fitting the experimental data by model-independent hyperfine-parameter distributions. α-Fe (red); Fe_3C (blue); Fe^{3+} in $(Al,Fe)_2O_3$ (green); γ-Fe–C (cyan). (For interpretation of the references to color in this figure legend, the reader is referred to the web version of the article.)

Table 2
Relevant hyperfine parameters for the components observed on the HTTMS spectra acquired at selected temperatures for the CNT–Fe–Al_2O_3 nanocomposite powder.

Temperature (°C)	$(Al,Fe)_2O_3$			α-Fe_2O_3				Fe^{2+} doublet		
	ΔE_Q	δ	RA	B_{hf}	$2\varepsilon_Q$	δ	RA	ΔE_Q	δ	RA
250	0.52	0.25	27	–	–	–	–	–	–	–
300	0.54	0.21	32	–	–	–	–	–	–	–
420	0.55	0.14	50	–	–	–	–	–	–	–
540	0.60	0.10	50	–	–	–	–	–	–	–
670	0.61	0.01	50	–	–	–	–	–	–	–
850	0.56	−0.04	59	–	–	–	–	–	–	–
25	0.57	0.31	31	50.9	−0.17	0.35	32	1.70	0.79[a]	7

Temperature (°C)	α-Fe			Fe_3C				γ-Fe–C	
	B_{hf}	δ	RA	B_{hf}	$2\varepsilon_Q$	δ	RA	δ	RA
250	31.3	−0.07	27	15.6	0.03	0.11	23	−0.22	23
300	31.0	−0.09	28	13.3	−0.01	0.14	19	−0.23	21
420	29.7	−0.15	29	–	–	–	–	−0.26	21
540	28.4	−0.21	30	–	–	–	–	−0.31	20
670	25.7	−0.27	30	–	–	–	–	−0.36	20
850	19.9	−0.24	21	–	–	–	–	−0.49	20
25	32.4	0.00	10	–	–	–	–	−0.14	20

B_{hf}: hyperfine field at maximum of the distribution (T); $2\varepsilon_Q$: quadrupole shifts (mm/s); ΔE_Q: quadrupole splitting at maximum distribution (mm/s); δ: isomer shifts (mm/s); RA: relative spectral areas (%). The values of isomer shifts are with reference to metallic iron.
[a] Fixed parameters.

doublet is obscured by and cannot be distinguished from the alumina doublet. This feature explains the concomitant changes in the RA values for the α-Fe sextet and the ferric doublet assigned to $(Al,Fe)_2O_3$ upon increasing the measuring temperature from 670 to 850 °C. Based on the well-known Néel-Brown expression [16,17] for the superparamagnetic relaxation time the size of the hematite particles is estimated to be around 25 nm.

The data of Table 3 indicate that the oxidation of Fe_3C gives rise to α-Fe_2O_3, as could be expected. The reason that no hematite sextet is observed in the HTTMS for temperatures $T \geq 250$ °C is believed to be the small size of the hematite particles and, as a consequence thereof, their superparamagnetic behaviour at temperatures exceeding some so-called blocking temperature. Evidence for the small particle size is provided by the low value of the magnetic hyperfine field for the hematite sextets in the room-temperature TMS spectra of the heated powders (Table 1—B_{hf} for bulk hematite is 51.7 T). When the temperature of the absorber is increased to a value higher than this blocking temperature, the Mössbauer event experiences a zero hyperfine field and the resulting spectrum has collapsed to a doublet with quadrupole splitting equal to the value corresponding to the paramagnetic state, i.e., a doublet which remains unresolved from the $(Al,Fe)_2O_3$ doublet.

Table 3
Some relevant relative spectral areas (in % of total spectrum area) obtained from the transmission Mössbauer spectra (TMS) collected at 25 °C for the CNT–Fe–Al_2O_3 nanocomposite powder after calcination in air at selected temperatures and as obtained from *in situ* high-temperature transmission Mössbauer spectra (HTTMS) collected at high temperatures of the CNT–Fe–Al_2O_3 nanocomposite powder. Estimated errors are ±2%.

Sample	TMS		HTTMS		
	RA_{ha}[a]	RA_c[b]	T (°C)	RA_a[c]	RA_c[b]
C0[d]	20	21	25	20	21
C250	29	16	250	27	23
C300	33	15	300	32	19
C420	41	7	420	50	–
C540	43	6	540	50	–
C670	51	–	670	50	–
C850	61	–	850	59	–

[a] Sum for hematite and alumina component.
[b] Cementite component.
[c] Alumina component.
[d] Results for parent non-calcined powder.

According to the results of Bodker and Morup [18] α-Fe_2O_3 particles with average particle size of 27 nm, which is about the size of the particles expected for the presently involved hematite phase, have a median blocking temperature of 70 °C. Such particles, if their size were rather uniform, which can be expected in the present case,

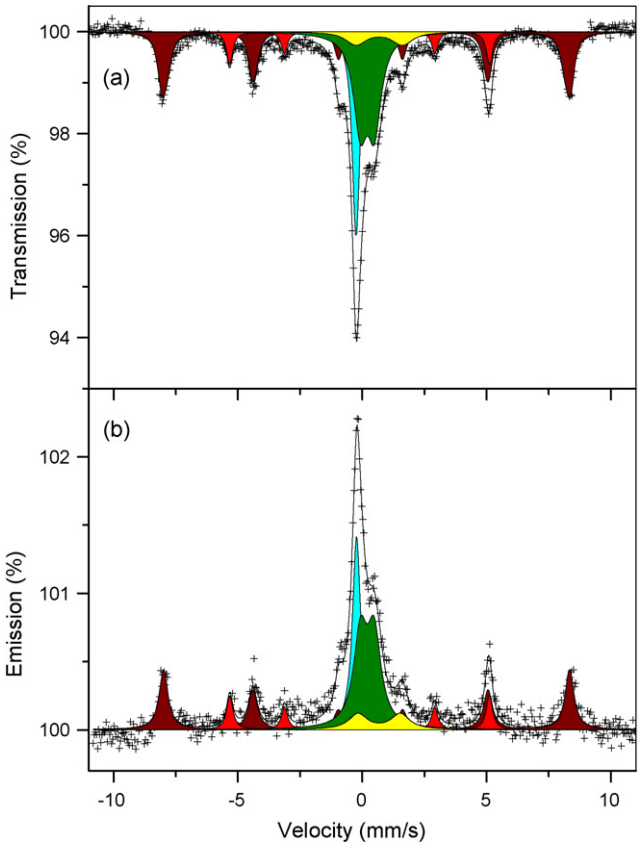

Fig. 8. TMS (a) and ILEEMS (b) spectra (at 25 °C) collected after the HTTMS measurements. Solid envelops are the results of fitting the experimental data by model-independent hyperfine-parameter distributions. α-Fe (red); α-Fe_2O_3 (brown); Fe^{3+} in $(Al,Fe)_2O_3$ (green); Fe^{2+} in $FeAl_2O_4$ (yellow); γ-Fe–C (cyan). (For interpretation of the references to color in this figure legend, the reader is referred to the web version of the article.)

would thus give rise to a well-defined sextet at 25 °C and a doublet at 250 °C or higher.

The absence of the Fe^{2+} due to $FeAl_2O_4$ phase in all of the HTTMS spectra is believed to be due to the weak contribution of this component (5% for sample C0, Table 1), which is then overlapped by the other components in the central part of the spectra.

After acquisition of the HTTMS at 850 °C and subsequent cooling down the sample to room temperature in air, its spectrum was again measured in TMS (Fig. 8a). The hyperfine parameters of the various components that could be resolved from that spectrum (Table 2) were found to be very similar to those obtained from the TMS for C850 (Table 1). An ILEEMS measurement at 25 °C for the powder resulting from HTTMS measurements was performed (Fig. 8b). The emission spectrum has the same shape and spectral components as does the HTTMS spectrum at 25 °C (Fig. 8a). The contributions of all components, i.e., hematite, α-Fe, γ-Fe–C, Fe^{3+} doublet and Fe^{2+} doublet are, within experimental errors limits, the same for the respective HTTMS and ILEEMS spectra indicating that all Fe-containing phases are evenly distributed between the bulk and the outer porosity on the one hand and at the surface of the grains on the other hand. It should be mentioned that the hyperfine parameters of all components obtained from the ILEEMS are within error limits identical to the values fitted to the HTTMS spectrum at 25 °C.

4. Conclusions

The thermal stability of a CNT–Fe–Al_2O_3 nanocomposite powder was studied using notably TGA and Mössbauer spectroscopy. In particular, *in situ* high-temperature transmission Mössbauer spectroscopy was performed for the first time on such materials. The oxidation process of the powder is characterized by several steps. The first weight gain (150–300 °C) was attributed to the oxidation into hematite (α-Fe_2O_3) of the α-Fe and Fe-carbide particles located at the surface and in the open porosity of the alumina grains, whereas a weight loss (300–540 °C) was thought to be the oxidation of carbon found as CNTs and graphene layers surrounding the Fe and Fe_3C particles. The formation of hematite was observed to start at about 250 °C. It was demonstrated that the hematite particles are superparamagnetic at temperatures equal to 250 °C or higher and were found to be approximately 25 nm in diameter. A remarkable aspect is that γ-Fe–C is unaffected even after oxidation at 850 °C. It was suggested that the encapsulation of γ-Fe–C particles by graphene layers leads to the stability of these particles, i.e. retention of γ (face-centered cubic) structure and in addition prevents them from oxidation. With the increase in calcination temperature, the graphene layers are oxidized and a very thin layer of α-Fe_2O_3 is formed at the surface of the γ-Fe–C particles, preventing the complete oxidation of the γ-Fe–C particles until at least 850 °C, while helping to retain the face-centered cubic structure. Finally, two successive weight gains at 670 and 1120 °C could correspond to the oxidation of the intragranular α-Fe particles and the γ-Fe–C particles.

Acknowledgements

This work was partially funded by the Fund for Scientific Research – Flanders, and by the Special Research Fund (*BOF, Bijzonder Onderzoeksfonds*), UGent (B/06633), Belgium. Electron microscopy observations were performed at TEMSCAN, the "Service Commun de Microscopie Electronique à Transmission", Université Paul Sabatier, Toulouse.

References

[1] Ch. Laurent, A. Peigney, A. Rousset, J. Mater. Chem. 8 (1998) 1263–1272.
[2] B. Kitiyanan, W.E. Alvarez, J.H. Harwell, D.E. Resasco, Chem. Phys. Lett. 317 (2000) 497–503.
[3] J.P.C. Trigueiro, G.G. Silva, R.L. Lavall, C.A. Furtado, S. Oliveira, A.S. Ferlauto, R.G. Lacerda, L.O. Ladeira, J.-W. Liu, R.L. Frost, G.A. George, J. Nanosci. Nanotechnol. 7 (2007) 3477–3486.
[4] A.W. Musumeci, G.G. Silva, W.N. Martens, E.R. Waclawik, R.L. Frost, J. Therm. Anal. Calorim. 88 (2007) 885–891.
[5] C.-W. Chang, J.-M. Tseng, J.-J. Horng, C.-M. Shu, Comp. Sci. Tech. 68 (2008) 2954–2959.
[6] H. Yu, C. Lu, T. Xi, L. Luo, J. Ning, C. Xiang, J. Therm. Anal. Calorim. 82 (2005) 97–101.
[7] Z. Konya, T. Kanyo, A. Hancz, I. Kiricsi, J. Therm. Anal. Calorim. 79 (2005) 567–572.
[8] V.G. de Resende, E. De Grave, A. Cordier, A. Weibel, A. Peigney, Ch. Laurent, Carbon 47 (2009) 482–492.
[9] E. De Grave, R.E. Vandenberghe, C. Dauwe, Hyperfine Interact. 161 (2005) 147–160.
[10] Ch. Laurent, Ch. Blaszczyk, M. Brieu, A. Rousset, Nanostruct. Mater. 6 (1995) 317–320.
[11] O. Quénard, Ch. Laurent, M. Brieu, A. Rousset, Nanostruct. Mater. 7 (1996) 497–507.
[12] X. Devaux, Ch. Laurent, M. Brieu, A. Rousset, J. Alloys Compd. 188 (1992) 179–181.
[13] H. Kim, W. Sigmund, J. Cryst. Growth 267 (2004) 738–744.
[14] V.G. de Resende, E. De Grave, A. Peigney, Ch. Laurent, J. Phys. Chem. C 112 (2008) 5756–5761.
[15] A. Van Alboom, E. De Grave, R.E. Vandenberghe, J. Solid State Chem. 95 (1991) 204–212.
[16] L. Néel, Ann. Geophys. 5 (1949) 99–136.
[17] W.F. Brown Jr., Phys. Rev. 130 (1963) 1677–1686.
[18] F. Bodker, S. Morup, Europhys. Lett. 52 (2000) 217–223.